

## Miscibility and surface crystal morphology of blends containing poly(vinylidene fluoride) by atomic force microscopy

Won-Ki Lee<sup>a</sup> and Chang-Sik Ha<sup>b,\*</sup>

<sup>a</sup>Research Institute of Industrial Technology, Pusan National University, Pusan, South Korea

<sup>b</sup>Department of Polymer Science & Engineering, Pusan National University, Pusan 609-735, South Korea

(Revised 30 August 1997)

The miscibility and surface crystalline structure of blends containing poly(vinylidene fluoride) (PVDF) composed of  $\alpha$  and  $\gamma$  phases were investigated by atomic force microscopy (AFM) and differential scanning calorimeter (d.s.c.) measurements. It was found that the surface crystalline phase of PVDF and the degree of surface enrichment of a lower surface free energy component in a blend might strongly be affected by the magnitude of the intermolecular interaction, even though the blend is miscible. Also, the segmental interaction parameters were determined by combining the  $T_m$  depression of PVDF in a blend and the binary interaction model. According to the binary interaction model, the introduction of a carboxyl group for miscible [poly(methyl methacrylate)/PVDF] and [poly(vinyl acetate)/PVDF] blends decreased their miscibility. © 1998 Elsevier Science Ltd. All rights reserved.

(Keywords: atomic force microscopy; surface crystalline structure; segmental interaction parameter)

### Introduction

Poly(vinylidene fluoride) (PVDF) crystallises in five different polymorphs,  $\alpha$ ,  $\beta$ ,  $\gamma$ ,  $\delta$  and  $\epsilon$ , and each crystal structure exhibits different polymorphs<sup>1</sup>. Among them, the  $\beta$  and  $\gamma$  phases of PVDF have recently attracted much interest, particularly in regard to piezo- and pyro-properties and the unit-cell structure<sup>2–4</sup>. PVDF has good mechanical strength and environmental resistance, but its poor optical clarity limits its use as an optical material. Although much emphasis has been placed on the blend with amorphous polymer to improve the optical property of PVDF<sup>5–7</sup>, little is known about their surface crystal phase.

On the other hand, the surface structure of polymer blends has attracted much interest because of the practical importance of the associated functional properties, such as lubricant, wetting, friction, and so on. It has been revealed that the surface structure of polymer blends is clearly different from that in the bulk, mainly depending on the difference in the surface free energy of each component<sup>8–11</sup>. The lower surface free energy component of a multiphase polymer blend is enriched at the surface in order to minimise the interfacial free energy. Also, it was reported that the crystallinity of homopolymer is enhanced at the surface<sup>12</sup>. This result is significant in light of the dramatic difference in properties between the crystalline and amorphous phases of a semi-crystalline polymer. To design a highly functionalised surface, therefore, it is necessary to understand molecular behaviour at the surface and to control surface properties.

In general, the miscibility of a blend including semi-crystalline components is achieved by the interaction between amorphous parts of each component. The  $T_m$  depression of a crystalline component means that the re-growth of a crystal is interrupted by the interaction between components in blend and can be used to estimate the interaction parameter  $B$  between components

in blend<sup>13,14</sup>.

$$T_m^\circ - T_m = -T_m^\circ \frac{B \cdot V_{2u}}{\Delta H_{2u}} \phi_1^2 \quad (1)$$

In equation (1), the subscript 1 and superscript 2 are the noncrystallisable and crystallisable components, respectively, and  $T_m^\circ$  and  $T_m$  are the equilibrium melting points of pure component 2 and 2 in a blend, respectively;  $\phi_1$  is volume fraction and  $\Delta H_{2u}/V_{2u}$  is the heat of fusion per unit volume of crystallisable component.

In this study, the surface crystalline morphology of PVDF and its miscibility with some polymers were studied using atomic force microscopy (AFM) and differential scanning calorimetry (d.s.c.) measurements. The surface morphology of these blends is expected to be strongly influenced by the difference of surface free energy and intermolecular interactions between their components used.

### Experimental

**Materials and film preparations.** PVDF used in this study was obtained from Showa Chemical Co. Polystyrene (PS) was from Aldrich. Poly(methyl acrylate) (PMA) homopolymer and poly(vinyl acetate-co-acetic acid) (poly(VAc-co-AA)) were synthesised by the radical polymerisation. Poly(methyl methacrylate) (PMMA,  $M_w = 120\,000$ ) was purchased from Aldrich. The characteristics of polymers in this study are listed in Table 1. The surface free energy,  $\gamma_{sv}$ , of polymers was estimated from the contact angle data using the method of Owens and Wendt<sup>15</sup>. The measurement were carried out in the presence of the saturated vapours of the probe liquids, water and methylene iodide. The precision in the contact angle measurements was 0.2° and 10 measurements were averaged with a confidence limit of 95%. PMMA was partially hydrolysed by dissolving PMMA in 96% sulphuric acid followed by stirring at room temperature for 30 and 72 h. The solutions were precipitated in an ice/water mixture, filtered, dissolved in water with KOH and heated to 373 K for 1 h to remove anhydride functionalities. The

\*To whom correspondence should be addressed

hydrolysed PMMA is a copolymer of methyl methacrylate (MMA) and methacrylic acid (MAA). The details for the synthesis were reported elsewhere<sup>16</sup>. The carboxyl group content of each polymer was confirmed by <sup>1</sup>H n.m.r. spectra. The AA content of poly(VAc-co-AA) was 8 mol.%. Each H-PMMA contains 14 and 24 mol.% of carboxyl groups and is designated by the degree of hydrolysis. For instance, H14-PMMA denotes that the carboxyl group in hydrolysed PMMA is 14 mol.%. Blends were prepared by dissolving respective components in dimethylacetamide (DMAc), followed by a casting method. The blend films were dried at 333 K. A blend composition of 50/50 was used in all cases.

#### Analytical methods

**Wide-angle X-ray diffractometry.** The crystalline structure of PVDF was determined using an X-ray diffractometer (Rigaku Denki). Nickel-filtered Cu K $\alpha$  radiation was applied at 30 kV and 20 mA.

**Transmission infrared spectroscopy.** The transmission FT-i.r. was taken with a Nicolet 1720X FTIR spectrometer. The data of 100 scans were averaged.

**Differential scanning calorimetry.** The  $T_m$  behaviours of PVDF homopolymer and blends, including PVDF, were measured by d.s.c. (Perkin-Elmer DSC 7) calibrated with pure indium as a standard. The PVDF homopolymer and blend samples were melted at 473 K for 10 min under dried helium purge, cooled quickly to the 433 K and kept at this temperature for 3 h. After isothermal crystallisation was finished, the samples were slowly cooled to room temperature, and then heated to 473 K at a heating rate of 20 K min<sup>-1</sup> for measuring  $T_m$  of PVDF.

**Atomic force microscopy.** Surface morphology was investigated by direct AFM observation. The AFM image was obtained using SPA 300 with SPI 3700 controllers (Seiko Instrument Co.) at room temperature (RT, 295 K). The cantilever used was microfabricated from Si<sub>3</sub>N<sub>4</sub> and its spring constant was 0.02 N m<sup>-1</sup>. AFM imaging was carried

out in a repulsive force. The scanning direction was horizontal to the long axis of the cantilever.

#### Results and discussion

Wide-angle X-ray diffractometry (WAXD) and i.r. measurements were performed to identify the crystalline phase of PVDF used in this study. *Figure 1* shows the X-ray diffraction pattern of the as-cast PVDF film. The WAXD pattern indicates that the PVDF of this work consists of a significant amount of the  $\alpha$  phase. From the X-ray diffraction, however, it is usually difficult to separate features arising from *trans* sequences in the  $\beta$  or  $\gamma$  forms<sup>17</sup>. *Figure 2* shows the i.r. spectrum of PVDF to obtain more information about the crystalline phase of PVDF. Even though the CF bending at 510 cm<sup>-1</sup> and the CH<sub>2</sub> rocking bands at 845 cm<sup>-1</sup> have been widely used to confirm the  $\beta$  structure, it would be more accurate to assign the 470-cm<sup>-1</sup> band as a characteristic  $\beta$  form<sup>1,18</sup>. The 815-, 776-, 510- and 430-cm<sup>-1</sup> bands are all assignable to the  $\gamma$  phase, and the bands, such as 965, 796 and 530 cm<sup>-1</sup> are considered as the  $\alpha$  phase. The i.r. results, therefore, show that PVDF used in this study is composed of  $\alpha$  and  $\gamma$  phases.

On the other hand, AFM is one of the new scanning probe microscopic techniques which became an important method to investigate the material surface morphology with high resolution<sup>19,20</sup>. *Figure 3* shows AFM topographic images of the semi-crystalline PVDF homopolymer film before and after annealing at 425 K for 10 min. The AFM images could clearly exhibit dendrite  $\alpha$  and spherulite  $\gamma$  phases. Since annealing was carried out above the  $T_m$  of the  $\alpha$  phase, the remaining crystalline phase might consist of mainly the  $\gamma$  phase, which was in the crystal form at that temperature. It was reported that the  $T_m$  of the  $\gamma$  phase is higher than that of the  $\alpha$  phase<sup>5,6</sup>. Considering that the crystal phase of PVDF at the surface can be easily observed by AFM measurement, AFM observation can give information on the surface morphological change due to the interaction when a blend is composed of crystalline polymer as one component.

*Figure 4* shows  $T_m$  behaviours of PVDF for (PMA/PVDF 50/50), (PS/PVDF 50/50) and (PVAc/PVDF 50/50) blend films. As expected, the degree of  $T_m$  depression of the

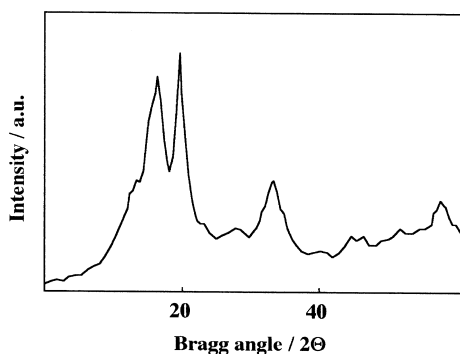


**Figure 1** X-ray diffractogram of as-cast PVDF homopolymer film

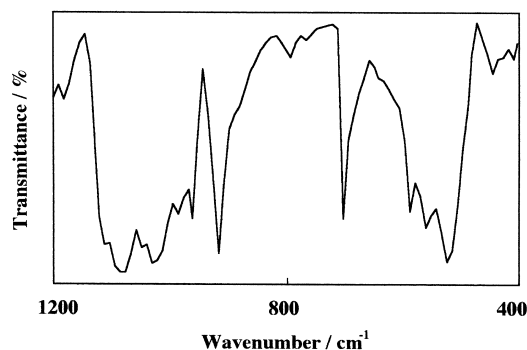


**Figure 2** I.r. spectrum of as-cast PVDF homopolymer film

**Table 1** Materials used in this study

Polymer	$M_w$	$M_w/M_n$	$T_g$ (K)	$T_m$ (K)	$\gamma_{sv}$ (mN m <sup>-1</sup> )
Poly(methyl acrylate) (PMA)	274 000	1.93	287	—	44.7
Poly(vinyl acetate) (PVAc)	79000	1.23	304	—	37.2
Poly(methyl methacrylate) (PMMA)	120 000	2.00	390	—	42.6
Poly(vinylidene fluoride) (PVDF)	320 000	2.10	—	423( $\alpha$ ), 433( $\gamma$ )	26.0

miscible blends, (PMA/PVDF) and (PVAc/PVDF), was larger than that of (PS/PVDF) blend which was immiscible in melt. The open and filled triangles indicate the depressed  $T_m$  of the  $\alpha$  and  $\gamma$  phases, respectively. It is noticeable that the  $T_m$  of the (PMA/PVDF) blend is much higher than that of the (PVAc/PVDF) blend, even though both polymer blends are miscible. This behaviour is more clear from their

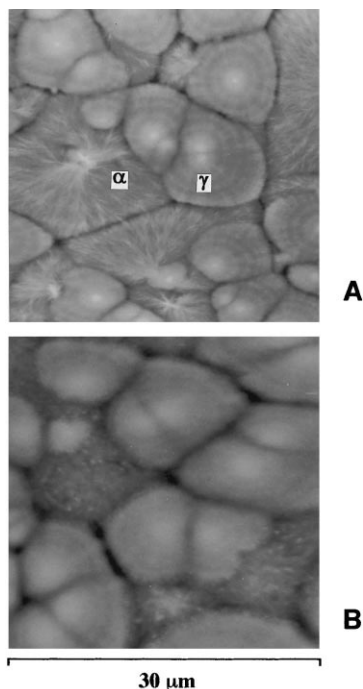


**Figure 3** AFM topographic images of PVDF homopolymer film. (A) As-cast; (B) after annealing at 425 K for 10 min

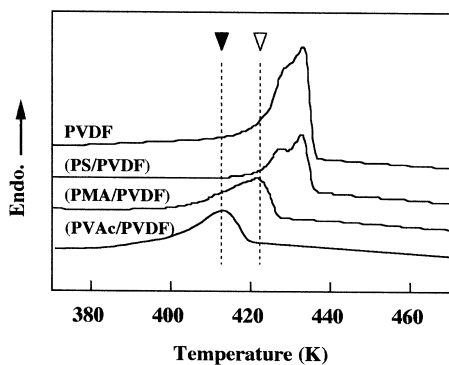


**Figure 4** D.s.c. thermograms for PVDF homopolymer and various PVDF-containing blends. The open and filled triangles indicate the depressed  $T_m$  values of  $\alpha$  and  $\gamma$  phases of PVDF due to the intermolecular interaction, respectively

**Table 2** Interaction parameter calculated by equation (1), and  $T_m$  behaviour of the  $\gamma$  crystalline phase of PVDF for various polymer blends

Blend system	$T_m$ (K)	$B$ (cal cm <sup>-3</sup> )	Crystalline phase <sup>a</sup>
PVDF homopolymer	423( $\alpha$ ), 433( $\gamma$ )	—	$\alpha, \gamma$
(PMMA/PVDF)	424	- 2.53	$\alpha, \gamma$
(H14-PMMA/PVDF)	429	- 1.13	$\alpha, \gamma$
(H24-PMMA/PVDF)	432	- 0.28	$\alpha, \gamma$
(PVAc/PVDF)	413 <sup><math>\alpha</math></sup>	- 2.88 <sup>b</sup>	$\alpha$
[poly(VAc-co-AA)/PVDF]	426	- 1.97	$\alpha, \gamma$

<sup>a</sup>Crystal phases were confirmed by AFM and d.s.c. measurements

<sup>b</sup>Calculated on the basis of  $T_m$  behaviour of a phase crystal

AFM images. *Figure 5* shows AFM images of (PMA/PVDF) and (PVAc/PVDF) blend films. In the case of a (PMA/PVDF) blend film, the surface is covered with  $\alpha$  and  $\gamma$  phases, whereas only  $\alpha$  phase is observed in (PVAc/PVDF) blend film at the surface. This might indicate that the formation of the  $\gamma$  phase of PVDF is hindered by mixing with PVAc. This result suggests that the crystal phase of PVDF could be controlled by the specific interaction when PVDF is mixed with a miscible amorphous polymer.

To investigate the effect of introduction of carboxyl group on the miscibility of (PMMA/PVDF) and (PVAc/PVDF) blend systems, d.s.c. measurement was performed. *Table 2* lists  $T_m$  behaviours of various polymer blends and interaction parameters,  $B$ , calculated by equation (1). It should be noted that equation (1) is applicable when  $T_m^*$  and  $T_{mb}^*$ (blend) are used. If non-equilibrium values of 'measured  $T_m$ ' are used, the morphological effect needs to be taken into consideration. Therefore, the 'experimental values of  $T_m$ (s)' were only used as an approximation in this calculation. It will be more appropriate to use their equilibrium values to calculate  $B$ . In this calculation, the  $\Delta H_{2u}$  and  $V_{2u}$  were 1600 cal mol<sup>-1</sup> and 36.4 cm<sup>3</sup> mol<sup>-1</sup>, respectively<sup>21</sup>. As the carboxyl content is increased,  $B$  is decreased, regardless of the blend system. This means that the addition of a carboxyl group for both blend systems decreases the miscibility. From  $B_{PVDF/PMMA}$ ,  $B_{PVDF/H14-PMMA}$  and  $B_{PVDF/24-PMMA}$  values,  $B$

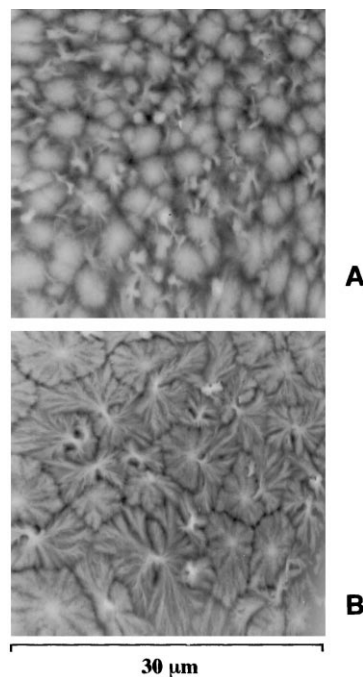


**Figure 5** AFM topographic images of (PMA/PVDF, 50/50, w/w) (A) and (PVAc/PVDF, 50/50, w/w) (B) blend films

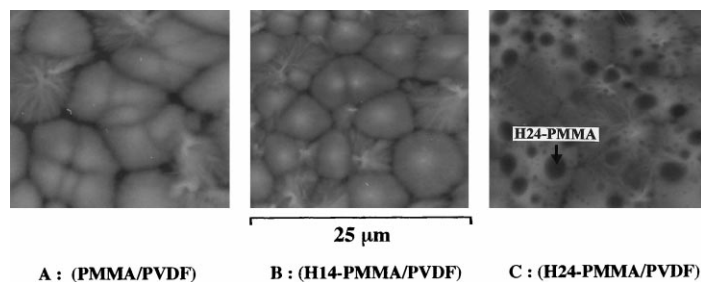


**Figure 6** AFM topographic images of (PMMA/PVDF, 50/50, w/w) (A), (H14-PMMA/PVDF, 50/50, w/w) (B) and (H24-PMMA/PVDF, 50/50, w/w) (C) blend films

between PVDF and poly(methacrylic acid) (PMAA) can be expressed as equation (2), by the general binary interaction model for the homopolymer/copolymer blends<sup>22</sup>.

$$B_{\text{PVDF/H-PMMA}} = \phi \cdot B_{\text{PVDF/PMMA}} + (1 - \phi) \cdot B_{\text{PVDF/PMAA}} - \phi \cdot (1 - \phi) \cdot B_{\text{PMMA/PMAA}} \quad (2)$$

where  $B_{\text{PVDF/PMAA}} = 2.53 \text{ cal cm}^{-3}$ , and  $B_{\text{PMMA/PMAA}} = -5.68 \text{ cal cm}^{-3}$ .

The positive value of  $B_{\text{PVDF/PMAA}}$  implies that the blend of PVDF and PMAA is immiscible, whereas the negative value of  $B_{\text{PMMA/PMAA}}$  indicates a miscibility between PMMA and PMAA. Table 2 also shows that the [poly(VAc-co-AA)/PVDF] blend exhibits both  $\alpha$  and  $\gamma$  crystalline phases, while the (PVAc/PVDF) blend exhibits only the  $\alpha$  phase. The result also implies that the miscibility of the (PVAc/PVDF) blend becomes weaker by incorporating a carboxyl group (here AA) into the blend system. Figure 6 shows AFM images of (PMMA/PVDF), (H14-PMMA/PVDF) and (H24-PMMA/PVDF) blend films. The surface free energy of H-PMMA was calculated as 43.6 and 44.4 mN m<sup>-1</sup> for H14-PMMA and H24-PMMA, respectively. (PMMA/PVDF) and (H14-PMMA/PVDF) blend film surfaces are fully covered with PVDF crystalline phases. In the case of the (H24-PMMA/PVDF) blend film surface, however, some defects were observed, aggregated H-PMMA domains, even though the surface free energy difference between PVDF and H-PMMA is increased as the carboxyl group in PMMA is increased. This phenomenon is not consistent with the general rule that the degree of surface enrichment of the lower surface free energy component for a multiphase polymer blend is mainly dependent on the differences in the surface free energy of components. The result suggests that the surface enrichment in this work is more strongly affected by the interaction parameter rather than the surface free energy differences. Therefore, it should be noted that the degree of surface enrichment is controlled by the combined factors of magnitude of interaction parameter and surface free energy difference, etc.

### Conclusions

The miscibility and surface crystalline structure of blends containing PVDF composed of  $\alpha$  and  $\gamma$  phases were investigated on the basis of AFM and d.s.c. measurements. Both  $\alpha$  and  $\gamma$  phases of PVDF were obtained upon blending with PMMA, H-PMMA and poly(VAc-co-AA). However, the  $\alpha$  form predominated in blending with PVAc. These results revealed that the crystalline phase of PVDF could be controlled by blending with an amorphous polymer having

the specific interaction with PVDF. Although the surface free energy difference with PVDF is increased with increasing carboxyl group content in PMMA, the H-PMMA domains were observed at the (H24-PMMA/PVDF) blend film surface, whereas the surface of (PMMA/PVDF) and (H14-PMMA/PVDF) blend films fully composed with PVDF crystals. It was then found that the degree of surface enrichment of multiphase polymer blends is more affected by the magnitude of interaction than the surface free energy difference between components. Also, the segmental interaction parameters were determined by combining the  $T_m$  depression of PVDF in blend and the binary interaction model. According to the binary interaction model, the addition of a carboxyl group for miscible (PMMA/PVDF) and (PVAc/PVDF) blends decreased their miscibility.

### Acknowledgements

The authors wish to thank Prof. T. Kajiyama and Prof. A. Takahara of Kyushu University for their help in AFM measurement.

### References

1. Lu, F.J. and Hsu, S.L., *Macromolecules*, 1986, **19**, 326.
2. Lovinger, A.J., *Macromolecules*, 1981, **41**, 322.
3. Hahn, B.R. and Wendorff, J.F., *Polymer*, 1985, **26**, 1619.
4. Su, J., Ma, Z.Y., Scheinbein, J.I. and Newman, B.A., *J. Polym. Phys., Polym. Phys.*, 1995, **33**, 85.
5. Roerdrink, E. and Challa, G., *Polymer*, 1978, **19**, 73.
6. Ward, T.C. and Lin, T.S., *Adv. Chem. Ser.*, 1981, **206**, 59.
7. Gan, P.P. and Paul, D.R., *Polym. Phys., Polym. Phys.*, 1995, **33**, 1693.
8. Thomas, H.R. and Malley, J.J., *Macromolecules*, 1979, **12**, 323.
9. Malley, J.J., Thomas, H.R. and Lee, G.M., *Macromolecules*, 1979, **12**, 997.
10. Russell, T.P., Hjelm, R.P. Jr. and Seeger, P.A., *Macromolecules*, 1990, **23**, 890.
11. Lee, W.K., Cho, W.J., Ha, C.S., Takahara, A. and Kajiyama, T., *Polymer*, 1995, **36**, 229.
12. Wu, W., Satija, S.K. and Majczak, C.F., *Polym. Commun.*, 1991, **32**, 363.
13. Nishi, T. and Wang, T.T., *Macromolecules*, 1975, **8**, 809.
14. Paul, D.R., Barlow, J.W., Bernstein, R.E. and Wchrmund, D.C., *Polym. Eng. Sci.*, 1978, **18**, 1225.
15. Owens, D.K. and Wendt, R.C., *J. Appl. Polym. Sci.*, 1969, **13**, 1741.
16. Brinkhuis, R.H.G. and Schouten, A.J., *Macromolecules*, 1992, **25**, 6173.
17. Yang, D.Y. and Tomas, E.L., *J. Mater. Sci. Lett.*, 1984, **3**, 929.
18. Suess, M., Kressler, J. and Kammer, H.W., *Polymer*, 1987, **28**, 957.
19. Ginnig, G., Quate, C.F. and Gerber, C.G., *Phys. Rev. Lett.*, 1986, **56**, 930.
20. Lee, W. K., Ha, C. S., *Kor. Polym. J.*, 1997, **5**, 2, 73.
21. Paul, D.R. and Barlow, J.W., *Polymer*, 1984, **25**, 387.
22. Nakagawa, K. and Ishida, Y.J., *Polym. Sci., Polym. Phys. Ed.*, 1973, **11**, 2153.